Hindawi
Journal of Food Processing and Preservation
Volume 2024, Article ID 6646949, 10 pages
https://doi.org/10.1155/2024/6646949

Research Article

Co-encapsulation of β-D-Galactosidase and Ascorbic Acid in the Milk Protein-Based Microcapsules: Optimization and Characterization

Mahmoud Hosseinnia, Mohammad Alizadeh Khaledabad, and Hadi Almasi

Department of Food Science and Technology, Faculty of Agriculture, Urmia University, Urmia, Iran

Correspondence should be addressed to Mohammad Alizadeh Khaledabad; malizadeh@outlook.com

Received 4 June 2023; Revised 24 January 2024; Accepted 7 March 2024; Published 4 April 2024

Academic Editor: Rafik Balti

This research is aimed at preparing the β-galactosidase (βg) and vitamin C (VC) cocapsules stabilized by milk proteins. The effect of different independent parameters including core-coating ratio (10-100%), whey protein isolate (0 : 1), sodium caseinate (0 : 1), and ultrasound power (50-150 W) on physicochemical properties of microcapsules was investigated. The response surface methodology (RSM) defined the optimal conditions. Increasing the WPI values had different effects on the particle size and polydispersity index (PDI). The zeta potential values decreased by decreasing SC values. The βg had better encapsulation efficiency in comparison to VC. Increasing the core-coating ratio showed a negative effect on the enzyme activity. Among the test parameters, the core-coating ratio was effective on the viscosity of microcapsules. Two optimum conditions for co-encapsulation were determined as WPI, SC, core-coating ratio, and ultrasound power of 0, 1, 100%, and 79.4 W and 0.2, 0.8, 100%, and 75 W for microcapsules I and II, respectively. In the next step, the structural and morphological properties of the optimum samples were analyzed. The heterogeneous morphology of microcapsules was observed by SEM analysis. The formation of new interactions between wall materials, βg, and VC was confirmed by FT-IR analysis. XRD analysis revealed that the WPI-coated sample had a higher crystallinity index. Generally, the successful co-encapsulation of βg and VC exhibited the potential of the resultant microcapsules for the industrial production of VC fortified and lactose-free milk.

1. Introduction

The name "lactose" comes from lac (meaning milk) and -ose to indicate that it is a sugar. It is more important in the dairy products [1]. Three-quarters of the world's people have lactose intolerance problems, which are caused by the inactivity of the lactase enzyme. Therefore, researchers have attended lactose-free and low-lactose foods in recent years. The authors of a study eliminate lactose intolerance and add encapsulated lactase enzyme to food products [2, 3]. The β-galactosidase enzyme is a helpful converter enzyme used to convert lactose to constituent units (glucose and galactose). Lactase is obtained from various sources, and *Kluyveromyces lactis* is a critical microbial source [4].

Vitamin C (*L*-ascorbic acid) has high antioxidant activity, which is vital for a healthy body. It is sensitive to heat and alkali substances. Foods containing vitamin C, such as functional beverages, prevent several diseases, such as cardiovascular diseases [5, 6].

There are many techniques for microencapsulation. Ultrasound-assisted method that works with high-intensity ultrasound waves is one of them. This method has been used to encapsulate different core materials [7, 8]. Ultrasonication power is one of the efficient process factors that affect the dispersion stability of nanoparticles [9, 10].

One of the important steps of microencapsulation is the selection of wall material. Whey proteins and sodium caseinate have received more attention as protein-based fat

substitutes in encapsulating bioactive components [11]. The high surface activity of WPI is caused by its use as a coating material in the encapsulation process [12]. The WPC or WPI encapsulates vitamins and enzymes in two states: alone or in combination with other biopolymers [13, 14]. Sodium caseinate (SC) is mainly prepared by purifying casein from fresh milk using an acid coagulation technique and the addition of sodium hydroxide to it. The main features of sodium caseinate are classified as good emulsifying, helpful stabilizing agents, high molecular weight, and high viscosity. This protein has been extensively used to encapsulate vitamins and enzymes [15, 16].

Several studies have been done on the encapsulation of lactase enzyme [4, 17, 18]. Also, researchers have investigated the properties of encapsulated vitamin C [19, 20]. However, there is no research on the co-encapsulation of these core materials. The major objective of this study was to evaluate the properties of β-galactosidase and ascorbic acid coencapsulated in sodium caseinate and WPI as wall materials. Furthermore, the synergistic effects of βg and VC were analyzed.

2. Materials and Methods

2.1. Materials. Lactase (β-galactosidase) from *Kluyveromyces lactis* (*K.L*) (Mayalact 2000, 2000 NLU/g) was obtained from Mayasan Food Industries A.S. Company. Vitamin C (ascorbic acid) with weight average molar mass (M_w) of 176.13 gr·mol^{-1} was purchased from Merck Co. (Darmstadt, Germany). WPI (85 g/100 g protein) and milk protein isolate (sodium caseinate) were purchased from Davisco Foods International (USA). All other regents were prepared by Sigma (Germany).

2.2. Experimental Design. The combined design was used to evaluate the effects of WPI (X_1), SC (X_2), CCR (X_3), and US power (X_4) on different responses of coencapsulated β-galactosidase and ascorbic acids such as PDI (Y_1), zeta potential (Y_2), encapsulation efficiency (Y_3), and lactase activity (Y_4). The results were calculated using the software Design-Expert version 13 (Stat-Ease, Minneapolis, MN, USA). The component, factors, and levels for the independent variables are given in Table 1.

Fitting the linear models was performed by regression analysis. The desirability function approach is used to obtain optimum conditions of microcapsules. Then, optimal cocapsules are prepared using variables. Afterward, their structural and morphological are analyzed using an advanced instrumental analyzer.

2.3. Co-encapsulation of Lactase Enzyme and Vitamin C by Ultrasonication Method. The co-encapsulation process was performed with a method optimized in our previous research with some modifications [21]. Hydrated solutions of WPI and SC (1% by weight) were obtained by mixing them with buffer solution (pH 7 ± 0.01) and distilled water, respectively. The aqueous solutions of wall materials were stirred using a magnetic stirrer (Ared, Velp Co, Italy) for 20 min. They were kept at refrigerator temperature for half a day to complete hydration. β-Galactosidase and ascorbic acid were added into the suspension of each biopolymer by laboratory overhead stirrer (Meditry Instrument Co., Ltd., China) at 2000 rpm for 15 min to achieve the core ratios of 10, 33, 55, 78, and 100%. The system was treated by an ultrasonic probe (NexTgen Lab500, Sinaptec, France). This sonicator has a titanium sonotrode with a diameter of 13 mm that was used for co-encapsulation. All samples were sonicated in a 250 ml beaker using ultrasonic powers of 50-150 W. The sonication time of 1 min was used at room temperature. After encapsulation, the samples were frozen at -50°C. The frozen samples were freeze-dried by Alpha 1-2 LDplus freeze dryer (Christ, Germany) at 0.007 atm for 48 h.

Table 1: Independent variables and their levels used in RSM.

Run	WPI (X_1)	SC (X_2)	Core-coating ratio (%) (X_3)	US power (W) (X_4)
1	0	1	55	150
2	0	1	100	50
3	1	0	55	100
4	0	1	100	117
5	1	0	40	150
6	0.5	0.5	32.5	100
7	0	1	10	117
8	0.5	0.5	70	50
9	1	0	10	100
10	0.75	0.25	100	50
11	1	0	100	117
12	0.5	0.5	32.5	100
13	1	0	40	50
14	0.5	0.5	10	50
15	1	0	100	83
16	0.25	0.75	70	117
17	0	1	70	83
18	0.5	0.5	70	50
19	0.5	0.5	10	150
20	0.5	0.5	70	150
21	0	1	40	50
22	0.5	0.5	32.5	100
23	0.5	0.5	100	100
24	0.75	0.25	100	150
25	0.25	0.75	100	150

2.4. Physicochemical Properties of Cocapsules

2.4.1. Measurement of Particle Size of the Cocapsules. Mean particle size and size distribution of prepared βg and VC cocapsules were determined by a dynamic light scattering (DLS) device (Nanotrac Wave, Microtrac, San Diego, USA). Before the size measurement, cocapsules were diluted with distilled water. This analysis was performed at room temperature.

2.4.2. Zeta Potential Measurement. The main purpose of this experiment is to determine the surface charge of particles dispersed in cocapsules. The Nanotrac Wave (Microtrac, San Diego, USA) instrument was used for the zeta potential measurement of samples. Firstly, 1 mL of samples was diluted 50 times with deionized water, and then, the samples were poured into the cell and put in the device. The ZP was determined at 25°C.

2.4.3. Encapsulation Efficiency of VC and βg. Measurement of the percentage of encapsulation efficiency of core materials within the microcapsules was the purpose of this experiment. Encapsulation efficiency (EE%) was measured according to Ozdemir et al. with some modifications [22]. Microcapsules were mixed into deionized water (1 : 20) in a glass beaker. Sonication of the mixture was performed by ultrasonic homogenizer (NexTgen Lab500, Sinaptec, France). Then, 10 mL of hexane was added to the mixture using a heating magnetic stirrer (Ared, Velp Co, Italy) for 20 min, followed by centrifugation (Hettich, Mikro 220R, Germany) at 13000 g for 5 min. The UV/vis spectrophotometer (Lambda 365, PerkinElmer, USA) was used for absorbance measurement of VC and βg at 293 and 256 nm (λ_{max}), respectively. Regarding the surface content, the Whatman filter paper was used to filtrate a mixture of samples and hexane. The absorbance was read at the mentioned wavelengths. Total βg and VC content were calculated using this linear equation obtained from the calibration curve: $A = 0.78\,C + 2.421 \times 10^{-3}$ ($R^2 = 0.9941$) and $A = 0.86\,C + 4.213 \times 10^{-3}$ ($R^2 = 0.9971$). The EE% was calculated using the following equation:

$$\text{Encapsulation efficiency}\,(\%) = \frac{\text{total } \beta\text{g (VC)} - \text{surface } \beta\text{g(VC)}}{\text{total } \beta\text{g (VC)}} \times 100. \quad (1)$$

2.4.4. Lactase Activity. The method of Zhang et al. was used to determine the lactase activity of cocapsules [23]. The supernatant of microcapsules (0.5 ml) was added to phosphate buffer solution (0.1 M) containing a solution of ortho-nitrophenyl-β-galactosidase (o-NPG). One unit (U) of βg activity was defined as the amount of enzyme hydrolyzing 1 μmol of ONPG in 1 min. The UV/vis spectrophotometer (Lambda 365, PerkinElmer, USA) was used for absorbance measurement at 420 nm as λ_{max} of o-NPG.

2.4.5. Viscosity Measurement. The viscosity of cocapsules was measured at 25°C and a concentration of 5% using an LVDV-2T Brookfield viscometer (USA). Spindle 21 is a tool which is connected to Brookfield viscometer and operated under 50 rpm until 2 min.

2.5. Structural and Morphological Characteristics of Cocapsules

2.5.1. Fourier Transform Infrared (FT-IR) Spectroscopy. The chemical structure of coating materials and freeze-dried cocapsules was obtained by an infrared spectrometer (Shimadzu, IRTracer-100, Japan). The sample preparation was performed by the potassium bromide (KBr) method. This analysis used a resolution of 4 cm^{-1} and a scanning range from 4000 to 400 cm^{-1}.

2.5.2. Scanning Electron Microscopy (SEM). The surface morphology of microcapsules was investigated by SEM. Freeze-dried cocapsules were studied under the scanning electron microscope (EVO 15, ZEISS, Germany) at an accelerating voltage of 10 kV.

2.5.3. Powder X-Ray Diffraction (XRD). XRD analysis with a diffractometer (XRD, Philips PW1730, Netherlands) with Cu-Kα irradiation source ($\lambda = 1.5418$ Å) is operated under 40 kV and 30 mA. This analysis is performed on pure wall materials and powders of prepared microcapsules. The scanning samples were achieved in a 2θ range (2–70°) with a scanning speed of 0.05° sec^{-1} at room temperature. The following equation was used for calculating the crystallinity index (CrI) [24]:

$$\text{CrI}(\%) = \left[\left(\frac{I_{002} - I_{\text{am}}}{I_{002}}\right)\right] \times 100, \quad (2)$$

where I_{002} is the maximum intensity of the crystal plane reflection and I_{am} is the maximum intensity of the X-ray scattering broad band due to the amorphous part of the sample (diffraction intensity at $2\theta = 18°$).

3. Results and Discussion

3.1. Particle Size. The average mean volume diameter ($D_{[4,3]}$) of microcapsules is presented in Figure 1. As shown in the figure, increasing the WPI in values higher than 0.5 caused to decrease in particle size. Increasing core coating at values higher than 65% caused a decrease in the $D_{[4,3]}$ cocapsules, but at ratios lower than 65%, its effect was different. About the effect of US power, the particle size of cocapsules is reduced in the powers more than 100 W and increased at lower than 100 W. The lowest diameter was achieved when SC was used as wall material, and the core-coating ratio was 100% (160 nm). The higher ability of SC to reduce the interfacial tension due to its emulsifying activity index related to the presence of hydrophobic and hydrophilic parts is a significant characteristic of protein-based biopolymers such as SC. Similar results were observed in comparing different WPI : CN ratios in the encapsulation of α-tocopherol [25]. Also, the particle size of α-tocopherol emulsions stabilized by WPI had results in agreement with over data [26].

Figure 2 shows the particle size distribution of cocapsules affected by WPI, SC, and core ratios. Unlike $D_{[4,3]}$, the PDI was increased by increasing the WPI. WPI with a higher emulsifying effect and lower molecular weight was able to reduce the polydispersity of SC-stabilized cocapsules. The core-coating ratio parameter had an inverse effect on the polydispersity index. The ultrasonication intensity had no significant effect on the PDI of cocapsules. The general

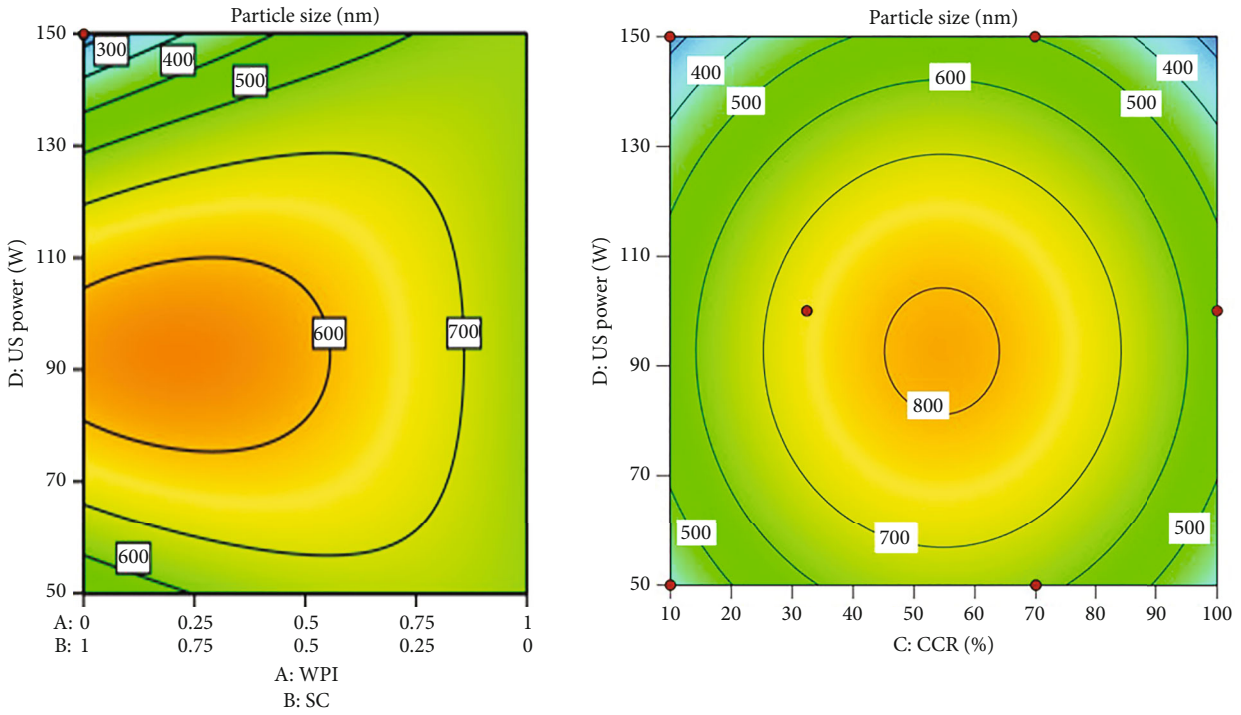

Figure 1: Counter plots of the effects of (A) WPI, (B) SC, (C) core-coating ratio, and (D) ultrasonic power on particle size of cocapsules.

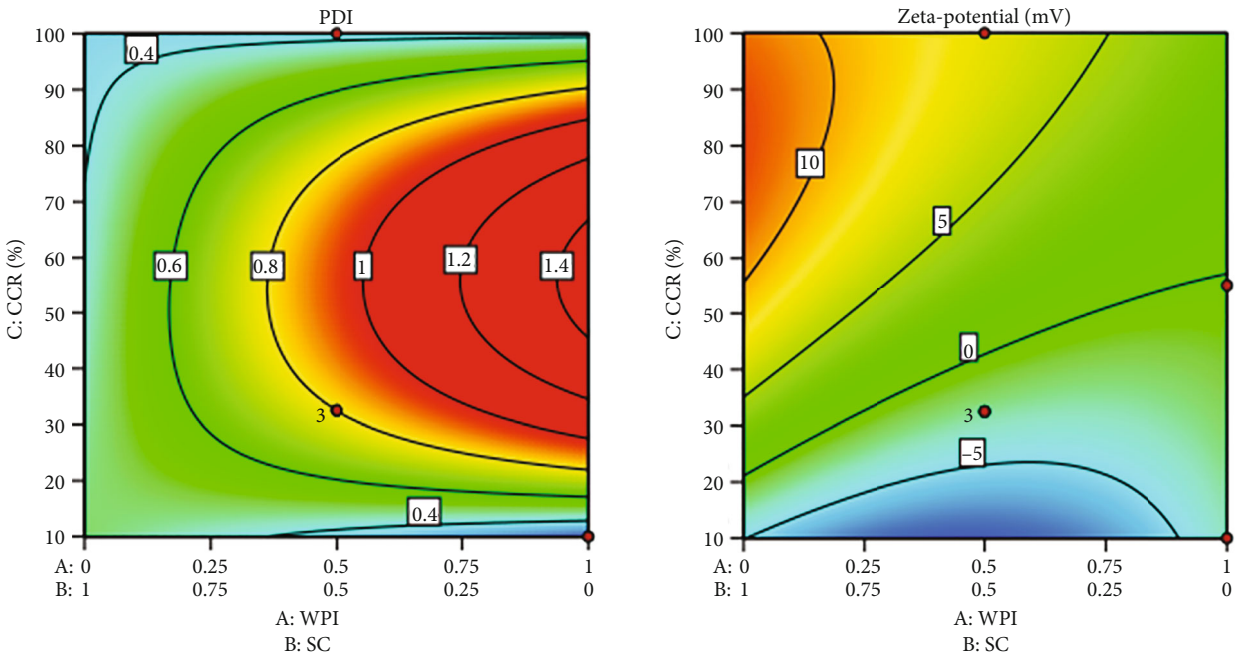

Figure 2: Counter plots of the effects of (A) WPI, (B) SC, and (C) CCR on PDI and zeta potential of microcapsules.

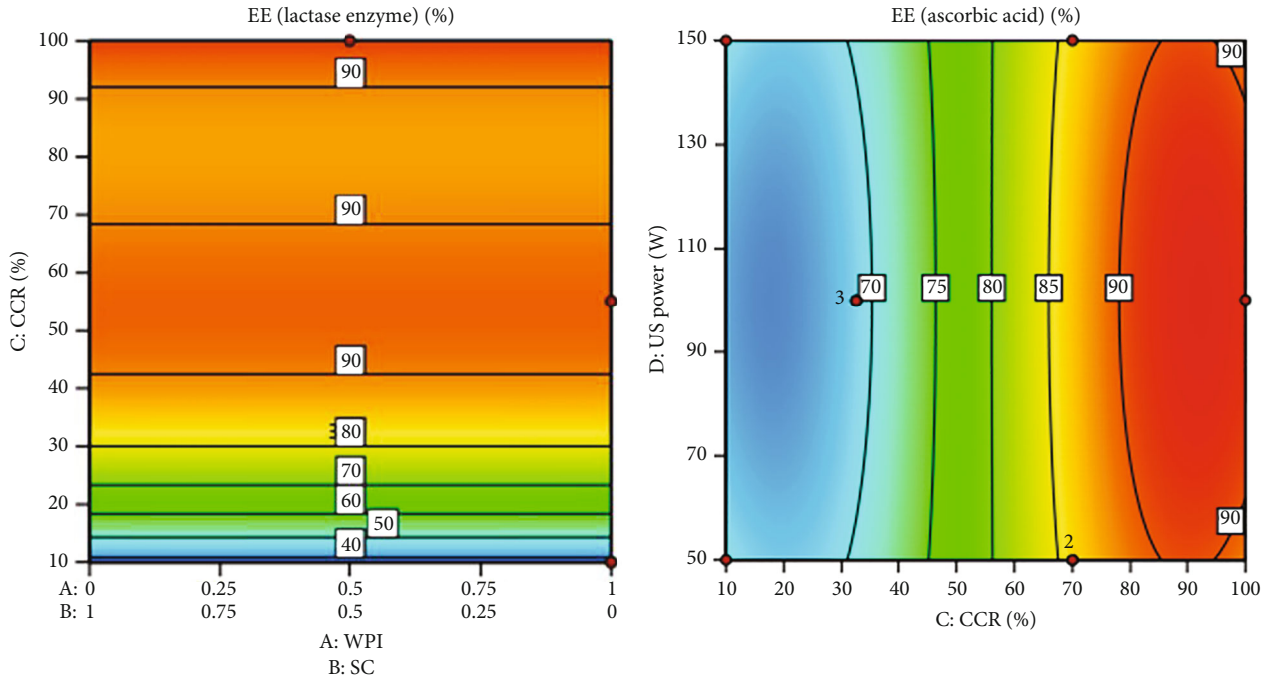

Figure 3: Counter plots of the effects of (A) WPI, (B) SC, (C) core-coating ratio, and (D) ultrasonic power on EE% of βg and VC cocapsules.

equations relating WPI, SC, CCR, US power to the particle size, and PDI are shown in

$$\begin{aligned}\text{Particle size (nm)} = {} & 38.86 * (\text{WPI}) - 841.031 \\ & * (\text{SC}) + 331.385 * (\text{WPI}) \\ & * (\text{SC}) + 19.379 * (\text{WPI}) \\ & * (\text{CCR}) + 8.905 * (\text{SC}) \\ & * (\text{CCR}) + 32.046 * (\text{SC}) \\ & * (\text{US power}) - 0.155 * (\text{WPI}) \\ & * (\text{CCR})^2 - 0.102 * (\text{SC}) \\ & * (\text{CCR})^2 - 0.172 * (\text{SC}) \\ & * (\text{US power})^2,\end{aligned} \tag{3}$$

$$\begin{aligned}\text{Polydispersity index} = {} & -0.324 * (\text{WPI}) + 0.47 * (\text{SC}) \\ & + 0.063 * (\text{WPI}) * (\text{CCR}) \\ & - 0.015 * (\text{SC}) * (\text{CCR}) + 0.007 \\ & * (\text{SC}) * (\text{US power}) + 0.00014 \\ & * (\text{SC}) * (\text{CCR}) * (\text{US power}) \\ & - 0.00057 * (\text{WPI}) \\ & * (\text{CCR})^2 - 0.00007 * (\text{SC}) \\ & * (\text{US power})^2.\end{aligned} \tag{4}$$

3.2. Zeta Potential. Zeta potential shows the net surface charge of microcapsules. Increasing zeta potential increases the kinetic stabilization of colloidal systems due to increasing electrostatic repulsion forces. Values presented in Figure 2 indicate the zeta potential of cocapsules. The zeta potential of samples decreased and increased by increasing WPI and core-coating ratios, respectively, since WPI and SC have pH isoelectric equal to 5. Therefore, the net charge of WPI and SC stabilized cocapsules was negative when the values were used in an equal value [27]. The zeta potential of cocapsules was not significantly affected by ultrasonication intensity. The zeta potential equation as a function of the studied parameters was mentioned as follows:

$$\begin{aligned}\text{Zeta potential (mV)} = {} & -3.673 * (\text{WPI}) - 10.028 * (\text{SC}) \\ & - 22.592 * (\text{WPI}) * (\text{SC}) + 0.064 \\ & * (\text{WPI}) * (\text{CCR}) + 0.545 * (\text{SC}) \\ & * (\text{CCR}) + 0.235 * (\text{WPI}) * (\text{SC}) \\ & * (\text{CCR}) - 0.003 * (\text{SC}) * (\text{CCR})^2.\end{aligned} \tag{5}$$

3.3. Encapsulation Efficiency of Core Materials. Figure 3 shows the EE values as a function of ultrasonic power, core ratios, WPI, SC, and core ratios for ascorbic acid and lactase enzyme emulsions, respectively. By comparing βg and VC, the EE% of βg in all of the microcapsules was higher than VC, but there was no statistically significant difference between them. Both WPI and SC have the emulsifying ability of amphiphilic. Like these results, Fu et al. reported EE without significant differences for coenzyme Q_{10}–vitamin E cocapsules [14]. The encapsulation efficiency of VC and βg increased by increasing the core-coating ratio. For both of them, the US power, WPI, and SC have no significant effect on the EE of emulsions. WPI and SC microparticles in equal

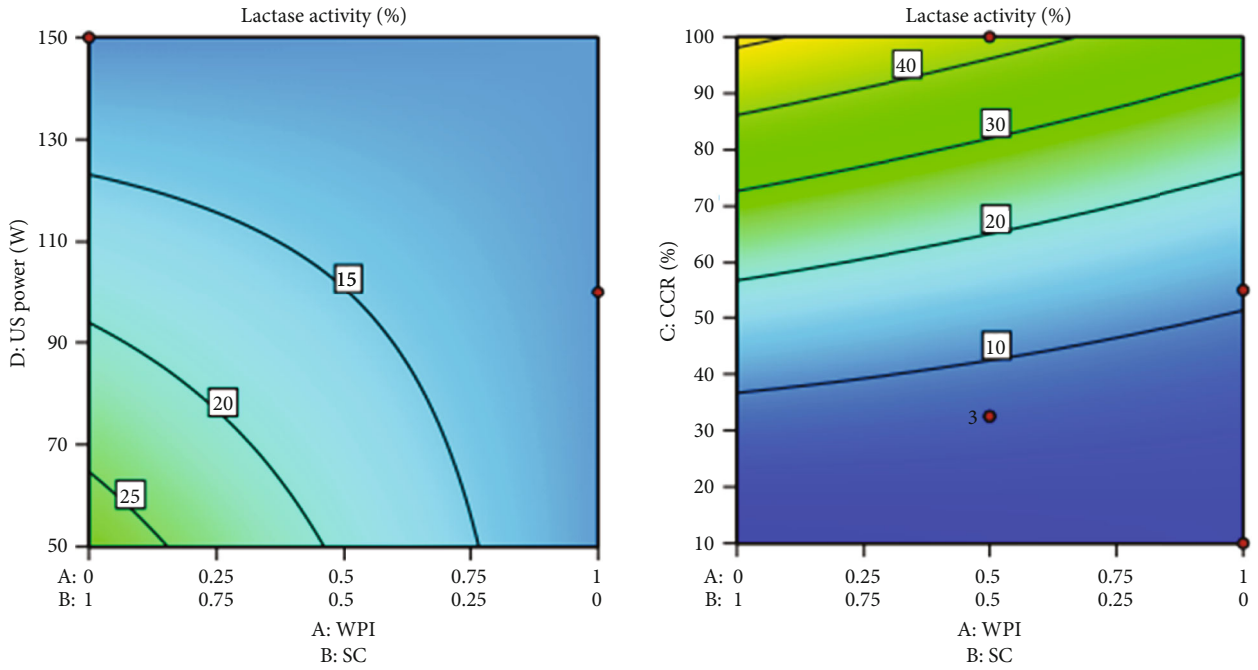

Figure 4: Counter plots of the effects of (A) WPI, (B) SC, (C) CCR, and (D) US power on the lactase activity of cocapsules stabilized by WPI and SC combinations.

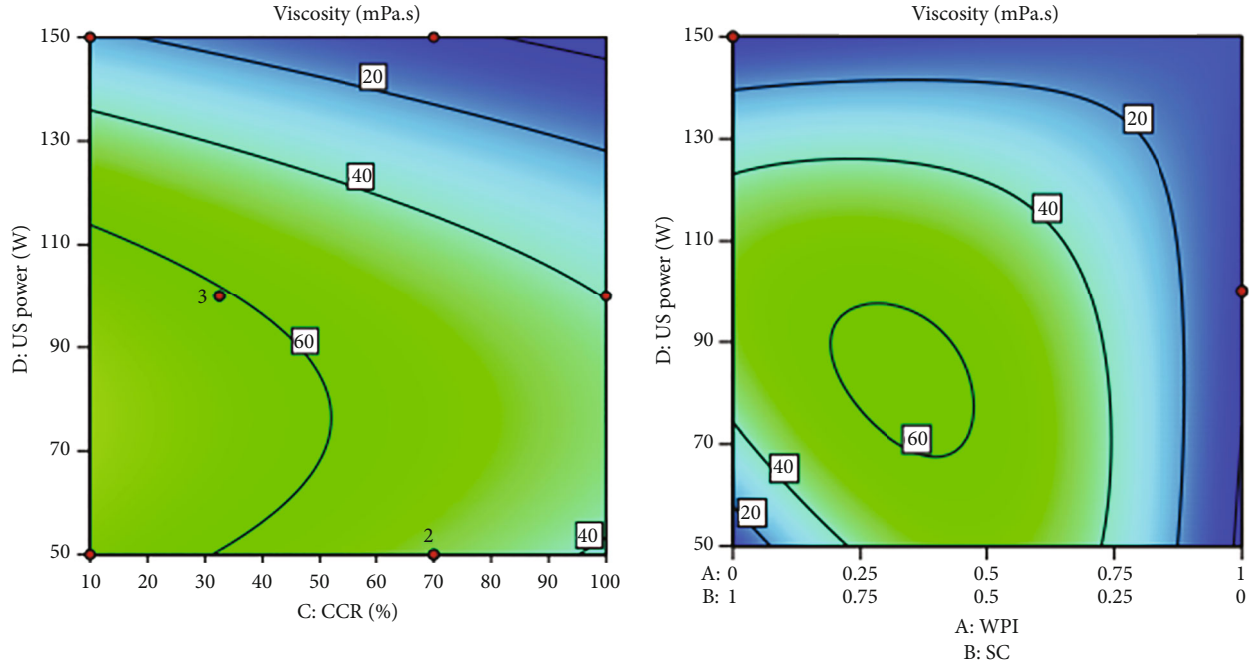

Figure 5: Counter plots of the effects of independent parameters on the viscosity of cocapsules stabilized by WPI and SC.

values showed the highest encapsulation efficiency value (99.2%). Khan et al. observed EE more than 95% for encapsulation of vitamin D with WPI and SPI. They stated that the highest EE was recorded when a 1 : 1 ratio of WPI and SPI was used [12]. EE values for lactase enzyme and ascorbic acid as a function of the US power and CCR were as follows:

$$\mathrm{EE}_{\mathrm{Lactase}}(\%) = -0.284 + 4.427 * (\mathrm{CCR}) - 0.068 * (\mathrm{CCR})^2 + 0.0003 * (\mathrm{CCR})^3, \quad (6)$$

$$\mathrm{EE}_{\mathrm{Ascorbic\ acid}}(\%) = 64.504 + 0.256 * (\mathrm{CCR}) + 0.0000001 * (\mathrm{CCR}) * (\mathrm{US\ power})^2 + 0.0000006 * (\mathrm{CCR})^3. \quad (7)$$

Table 2: Optimum microencapsulation conditions of βg/VC stabilized by WPI and SC.

Factor name	Goal	Optimized value		Desirability (%)	
		Microcapsule I	Microcapsule II	Microcapsule I	Microcapsule II
A: WPI	In range	0	0.2	100	100
B: SC	In range	1	0.8	100	100
C: core/coating ratio (%)	In range	100	100	100	100
D: US power (W)	In range	79.4	75	100	100
Particle size (nm)	Minimize	479.98	501.7	59	56.21
PDI	Minimize	0.185	0.185	100	100
Zeta potential (mV)	Maximize	11.18	9.66	88.99	82.31
EE (lactase enzyme) (%)	Maximize	94.87	94.87	93.76	93.76
EE (ascorbic acid) (%)	Maximize	91.13	90.91	94.67	93.95
Lactase activity (%)	Maximize	55.21	51.62	83.47	77.93
Viscosity (mPa·s)	None	16	34.73	100	100

Table 3: R^2, adjusted R^2, and predicted R^2 of the different responses.

Factor name	R^2	Adjusted R^2	Predicted R^2
Particle size (nm)	0.71	0.55	0.39
PDI	0.86	0.79	0.64
Zeta potential (mV)	0.94	0.92	0.89
EE (lactase enzyme) (%)	0.94	0.93	0.91
EE (ascorbic acid) (%)	0.91	0.9	0.88
Lactase activity (%)	0.9	0.88	0.85
Viscosity (mPa·s)	0.59	0.41	0.25

3.4. Influence of Co-encapsulation on β-Galactosidase Activity. Figure 4 shows βg activity curves as a function of core ratios, ultrasonic power, WPI, and SC. The βg activity had a direct proportion with core ratios. Unlike the core-coating ratio, the βg activity decreased by increasing the WPI and US power. Among the samples, the cocapsule containing SC as wall material with a high core ratio and ultrasonic power equal to 50 W had the highest enzyme activity value. Weng et al. stated that the storage stability of the encapsulated enzyme caused to increase the enzyme activity of microcapsules [28]. The enzyme activity was modeled as follows:

$$\begin{aligned}\text{Lactase activity}\,(\%) = {} & 3.674 * (\text{WPI}) + 16.785 \\ & * (\text{SC}) - 0.07 * (\text{WPI}) \\ & * (\text{CCR}) + 0.143 * (\text{SC}) \\ & * (\text{CCR}) - 0.171 * (\text{SC}) \\ & * (\text{US power}) + 0.003 * (\text{CCR})^2.\end{aligned} \tag{8}$$

3.5. Viscosity. The effects of ultrasonic power, CCR, WPI, and SC on the viscosity of cocapsules are shown in Figure 5. The viscosity of microcapsules is inversely proportional to the core-coating ratio. The lower molecular weight of core materials compared to wall materials caused to reduce viscosity. Increasing of WPI in values lower and higher than 0.5 caused to increase and decrease in viscosity, respectively. Data analysis showed that US power's effects around 100 W are similar to the WPI around 0.5. Data analysis of viscosity is shown in

$$\begin{aligned}\text{Viscosity}\,(\text{mPa}\cdot\text{s}) = {} & -10.194 * (\text{WPI}) - 96.078 * (\text{SC}) \\ & + 300.174 * (\text{WPI}) * (\text{SC}) + 0.138 \\ & * (\text{WPI}) * (\text{US power}) - 0.625 \\ & * (\text{SC}) * (\text{CCR}) + 3.679 * (\text{SC}) \\ & * (\text{US power}) - 1.942 * (\text{WPI}) \\ & * (\text{SC}) * (\text{US power}) - 0.018 \\ & * (\text{SC}) * (\text{US power})^2.\end{aligned} \tag{9}$$

3.6. Optimization and Desirability. Data optimization is made by the desirability function approach. The optimum values of wall materials, CCR, and US power were obtained by statistical analysis of results. These values and predicted values of dependent variables at optimum conditions are given in Table 2. Also, R^2, adjusted R^2, and predicted R^2 are given in Table 3. Predicting values of particle size (479.98 nm for microcapsule I and 501.7 nm for microcapsule II) was obtained when the optimum values of WPI, SC, CCR, and ultrasonication power were 0, 1, 100%, and 79.4 W and 0.2, 0.8, 100%, and 75 W for microcapsules I and II, respectively. Desirability values were equal to 0.83 and 0.797 for microcapsules I and II, respectively. Then, optimal cocapsules were prepared according to

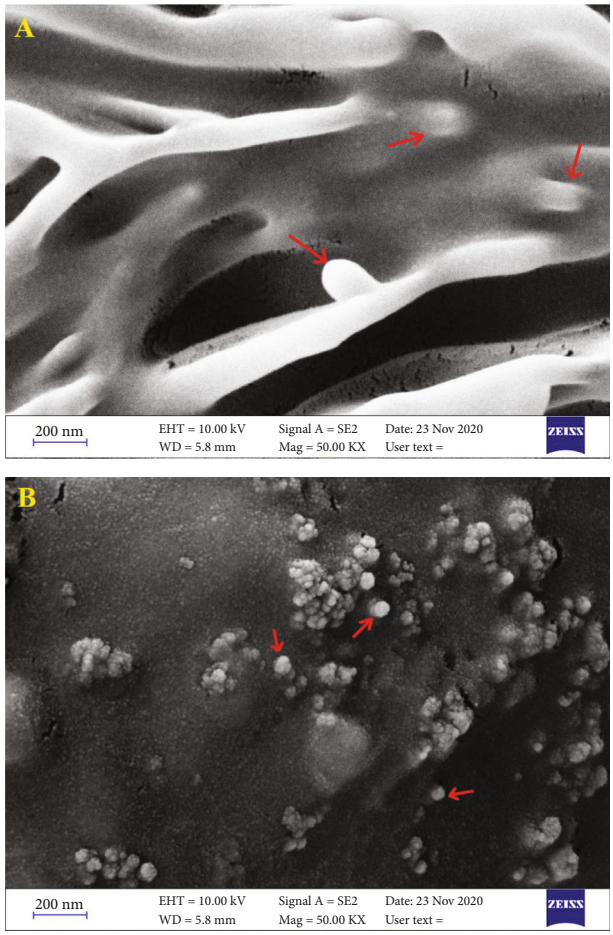

Figure 6: SEM images of βg and VC cocapsules stabilized by (a) SC and (b) WPI and SC under optimized conditions.

the defined objectives, and their structural properties were studied.

3.7. Morphology Observation by SEM. The size, shape, and morphology of microcapsules are noticeable in SEM images presented in Figure 6. There are no cracks on the surface of microparticles to indicate complete coverage of the wall material over the core and the successfulness of the encapsulation process. A significant reason for this achievement is the use of the freeze-drying method which works in lower temperatures. Parthasarathi and Anandharamakrishnan prepared vitamin E-loaded WPI microcapsules by three drying methods [29]. They stated that the freeze-drying method's shape uniformity and encapsulation efficiency are higher than other methods, because the freeze-drying process prevents from the creation of cracks and undesirable forms on the surface of capsules. The individual capsules are shown by arrows in the figures. As can be seen, more uniform and smooth morphology was obtained when SC was used as wall material. The heterogeneity increased, and rougher surface was achieved when SC and WPI were used as wall material. The average size of particles and size distribution has different values. The smallest particle size with uniform distribution was assigned to SC/WPI-stabilized microcapsules.

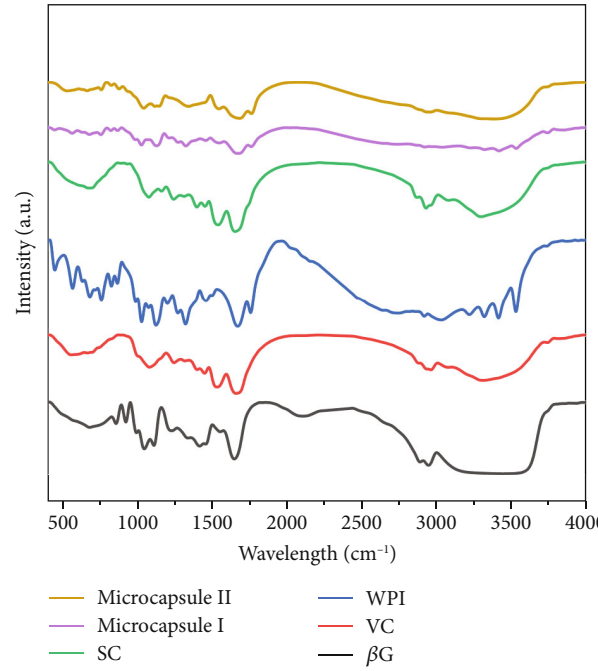

Figure 7: FT-IR spectra of βg, VC, pure WPI powder, pure SC powder, and microcapsules I and II.

3.8. FT-IR Spectroscopy. FT-IR curves of βg enzyme, VC, pure powder coatings (WPI and SC), and optimized βg-VC cocapsules are shown in Figure 7. The peaks between 3600 and 3200 cm^{-1} for βg are related to the vibration modes of O–H and N-H groups in the enzyme. The peak observed at 1650 cm^{-1} was attributed to the amide II of the enzyme [4]. As we reported in our previous research, several specific absorption peaks are related to pure WPI powder. C-N, N-H, C=O, C-H, and O-H bonds appeared at 667 cm^{-1}, 1075-1458 cm^{-1}, 1652 cm^{-1}, 1703 cm^{-1}, 3010 cm^{-1}, and 3500 cm^{-1}, respectively [21]. The spectra of pure SC showed the bands of C-O and COO- stretching at 1076 and 1390 cm^{-1}, respectively. N-H bonds were observed at 3308 cm^{-1}, recorded as a sharp peak. The peaks at 1644 and 1530 cm^{-1} are attributed to the amide type I and type II and asymmetrical C=O vibration [30]. As shown in Figure 7, the spectra of microcapsules changed substantially in comparison to pure materials. The intensity of the peaks related to –OH groups at 3600 cm^{-1} decreased, and the C-O and COO- stretching bonds at 1076 and 1390 cm^{-1} disappeared. These changes confirm that the βg and VC have chemically interacted with wall materials. Similar results were reported by Souza et al. and Silva et al. [4, 31].

3.9. XRD Analysis. Figure 8 shows the XRD patterns of pure coating materials and their optimized cocapsules. A typical amorphous structure is observed by XRD results for pure SC and WPI, with a broad peak at around 9° and 19°. The crystallinity index (CrI) for WPI and SC was computed at 26.5% and 20.13%, respectively. These data are similar to XRD results recorded for WPI and SC [32]. According to the curves, there are a lot of crystalline solid peaks in cocapsules' diffractograms. Creation of new interactions and chemically attachment of wall materials to the βg and VC

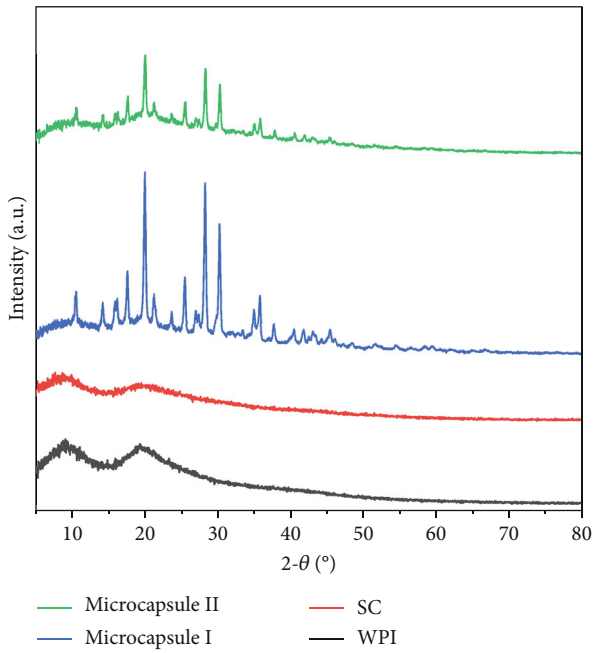

Figure 8: XRD patterns of pure hydrocolloids and microcapsules I and II.

is able to create new crystalline domains and thus leads to increase in crystallinity of cocapsules. Similar results were reported by Khan et al. and Ke et al. [12, 33].

4. Conclusions

This work evaluated the properties of β-galactosidase and ascorbic acid cocapsules. The RSM method is used to determine optimum values of WPI, SC, core ratio, and ultrasonication power. Smaller cocapsules were obtained when SC was used as wall material. A higher EE% was observed for βg in comparison to VC. The effect of independent variables such as core-coating ratio on lactase activity differed from viscosity values. The successful production of microcapsules with WPI and SC was confirmed by SEM images. IR analysis verified the observation of new interactions between coating materials and core material ingredients. Nevertheless, the XRD test indicated that these interactions lead to changes in the structural characteristics of biopolymers. In general, this research indicated that the βg and VC are able to encapsulate successfully in SC and WPI wall materials and the resultant cocapsules can be used for simultaneous VC fortification and lactose content reduction in milk.

Data Availability

All data are available upon request.

Conflicts of Interest

The authors certify that they have no affiliations with or involvement in any organization or entity with any financial interest (such as honoraria; educational grants; participation in speaker bureaus; membership, employment, consultancies, stock ownership, or other equity interest; and expert testimony or patent-licensing arrangements), or nonfinancial interest (such as personal or professional relationships, affiliations, knowledge, or beliefs) in the subject matter or materials discussed in this manuscript.

References

[1] M. S. Facioni, B. Raspini, F. Pivari, E. Dogliotti, and H. Cena, "Nutritional management of lactose intolerance: the importance of diet and food labelling," *Journal of Translational Medicine*, vol. 18, no. 1, p. 260, 2020.

[2] R. Catanzaro, M. Sciuto, and F. Marotta, "Lactose intolerance: an update on its pathogenesis, diagnosis, and treatment," *Nutrition Research*, vol. 89, pp. 23–34, 2021.

[3] E. Selvarajan, A. Nivetha, C. Subathra Devi, and V. Mohanasrinivasan, "Nanoimmobilization of β-galactosidase for lactose-free product development," *Nanoscience and Biotechnology for Environmental Applications*, vol. 22, pp. 199–223, 2019.

[4] C. J. F. Souza, T. A. Comunian, M. G. C. Kasemodel, and C. S. Favaro-Trindade, "Microencapsulation of lactase by W/O/W emulsion followed by complex coacervation: effects of enzyme source, addition of potassium and core to shell ratio on encapsulation efficiency, stability and kinetics of release," *Food Research International*, vol. 121, pp. 754–764, 2019.

[5] S. Q. Zhang, J. Li, L. Li, X. Yuan, L. Xu, and Z. G. Shi, "Fast separation of water-soluble vitamins by hydrophilic interaction liquid chromatography based on submicrometer flow-through silica microspheres," *Food Chemistry*, vol. 307, article 125531, 2020.

[6] J. Fraj, L. Petrović, L. Đekić, J. M. Budinčić, S. Bučko, and J. Katona, "Encapsulation and release of vitamin C in double W/O/W emulsions followed by complex coacervation in gelatin-sodium caseinate system," *Journal of Food Engineering*, vol. 292, article 110353, 2021.

[7] C. Gong, M. C. Lee, M. Godec, Z. Zhang, and A. Abbaspourrad, "Ultrasonic encapsulation of cinnamon flavor to impart heat stability for baking applications," *Food Hydrocolloids*, vol. 99, article 105316, 2020.

[8] D. Wang, M. Zhong, Y. Sun et al., "Effects of pH on ultrasonic-modified soybean lipophilic protein nanoemulsions with encapsulated vitamin E," *LWT*, vol. 144, article 111240, 2021.

[9] E. Huang, S. Y. Quek, N. Fu, W. D. Wu, and X. D. Chen, "Co-encapsulation of coenzyme Q10 and vitamin E: a study of microcapsule formation and its relation to structure and functionalities using single droplet drying and micro-fluidic-jet spray drying," *Journal of Food Engineering*, vol. 247, pp. 45–55, 2019.

[10] N. Zheng, L. Wang, and Z. Sun, "The effects of ultrasonication power and time on the dispersion stability of few-layer graphene nanofluids under the constant ultrasonic energy consumption condition," *Ultrasonics Sonochemistry*, vol. 80, article 105816, 2021.

[11] M. Yashini, C. K. Sunil, S. Sahana, S. D. Hemanth, D. V. Chidanand, and A. Rawson, "Protein-based fat replacers–a review of recent advances," *Food Reviews International*, vol. 37, no. 2, pp. 197–223, 2021.

[12] W. A. Khan, M. S. Butt, I. Pasha, and A. Jamil, "Microencapsulation of vitamin D in protein matrices: in vitro release and

storage stability," *Journal of Food Measurement and Characterization*, vol. 14, no. 3, pp. 1172–1182, 2020.

[13] A. Alehosseini, M. Sarabi-Jamab, B. Ghorani, and R. Kadkhodaee, "Electro-encapsulation of Lactobacillus casei in high-resistant capsules of whey protein containing transglutaminase enzyme," *LWT*, vol. 102, pp. 150–158, 2019.

[14] N. Fu, Y. J. You, S. Y. Quek, W. D. Wu, and X. D. Chen, "Interplaying effects of wall and core materials on the property and functionality of microparticles for co-encapsulation of vitamin E with coenzyme Q10," *Food and Bioprocess Technology*, vol. 13, no. 4, pp. 705–721, 2020.

[15] J. Mujica-Álvarez, O. Gil-Castell, P. A. Barra et al., "Encapsulation of vitamins A and E as spray-dried additives for the feed industry," *Molecules*, vol. 25, no. 6, p. 1357, 2020.

[16] J. Liu, Y. Zhang, S. He et al., "Microbial transglutaminase-induced cross-linking of sodium caseinate as the coating stabilizer of zein nanoparticles," *LWT*, vol. 138, article 110624, 2021.

[17] M. A. Cargnin, B. C. Gasparin, D. dos Santos Rosa, and A. T. Paulino, "Performance of lactase encapsulated in pectin-based hydrogels during lactose hydrolysis reactions," *LWT*, vol. 150, article 111863, 2021.

[18] L. Dong and Q. Zhong, "Dispersible biopolymer particles loaded with lactase as a potential delivery system to control lactose hydrolysis in milk," *Journal of Agricultural and Food Chemistry*, vol. 67, no. 23, pp. 6559–6568, 2019.

[19] J. Baek, M. Ramasamy, N. C. Willis, D. S. Kim, W. A. Anderson, and K. C. Tam, "Encapsulation and controlled release of vitamin C in modified cellulose nanocrystal/chitosan nanocapsules," *Current Research in Food Science*, vol. 4, pp. 215–223, 2021.

[20] B. Yan, S. M. Davachi, R. Ravanfar et al., "Improvement of vitamin C stability in vitamin gummies by encapsulation in casein gel," *Food Hydrocolloids*, vol. 113, article 106414, 2021.

[21] M. Hosseinnia, M. A. Khaledabad, and H. Almasi, "Optimization of *Ziziphora clinopodiodes* essential oil microencapsulation by whey protein isolate and pectin: a comparative study," *International Journal of Biological Macromolecules*, vol. 101, pp. 958–966, 2017.

[22] N. Ozdemir, A. Bayrak, T. Tat, F. Altay, M. Kiralan, and A. Kurt, "Microencapsulation of basil essential oil: utilization of gum Arabic/whey protein isolate/maltodextrin combinations for encapsulation efficiency and in vitro release," *Journal of Food Measurement and Characterization*, vol. 15, no. 2, pp. 1865–1876, 2021.

[23] Z. Zhang, R. Zhang, L. Chen, and D. J. McClements, "Encapsulation of lactase (β-galactosidase) into κ-carrageenan-based hydrogel beads: impact of environmental conditions on enzyme activity," *Food Chemistry*, vol. 200, pp. 69–75, 2016.

[24] A. Sarkar, D. R. Biswas, S. C. Datta et al., "Preparation of novel biodegradable starch/poly (vinyl alcohol)/bentonite grafted polymeric films for fertilizer encapsulation," *Carbohydrate Polymers*, vol. 259, article 117679, 2021.

[25] W. Xu, K. Lv, W. Mu, S. Zhou, and Y. Yang, "Encapsulation of α-tocopherol in whey protein isolate/chitosan particles using oil-in-water emulsion with optimal stability and bioaccessibility," *LWT*, vol. 148, article 111724, 2021.

[26] Z. Fang, X. Xu, H. Cheng, J. Li, C. Guang, and L. Liang, "Comparison of whey protein particles and emulsions for the encapsulation and protection of α-tocopherol," *Journal of Food Engineering*, vol. 247, pp. 56–63, 2019.

[27] H. Cheng, Q. Fan, T. Liu, Wusigale, and L. Liang, "Co-encapsulation of α-tocopherol and resveratrol in oil-in-water emulsion stabilized by sodium caseinate: impact of polysaccharide on the stability and bioaccessibility," *Journal of Food Engineering*, vol. 264, article 109685, 2020.

[28] Y. Weng, Y. Li, X. Chen, H. Song, and C. X. Zhao, "Encapsulation of enzymes in food industry using spray drying: recent advances and process scale-ups," *Critical Reviews in Food Science and Nutrition*, pp. 1–18, 2023.

[29] S. Parthasarathi and C. Anandharamakrishnan, "Enhancement of oral bioavailability of vitamin E by spray-freeze drying of whey protein microcapsules," *Food and Bioproducts Processing*, vol. 100, pp. 469–476, 2016.

[30] H. R. Kavousi, M. Fathi, and S. A. H. Goli, "Novel cress seed mucilage and sodium caseinate microparticles for encapsulation of curcumin: an approach for controlled release," *Food and Bioproducts Processing*, vol. 110, pp. 126–135, 2018.

[31] R. C. Silva, M. G. Trevisan, and J. S. Garcia, "β-galactosidase encapsulated in carrageenan, pectin and carrageenan/pectin: comparative study, stability and controlled release," *Anais da Academia Brasileira de Ciências*, vol. 92, no. 1, article e20180609, 2020.

[32] W. Liu, X. D. Chen, Z. Cheng, and C. Selomulya, "On enhancing the solubility of curcumin by microencapsulation in whey protein isolate via spray drying," *Journal of Food Engineering*, vol. 169, pp. 189–195, 2016.

[33] P. Ke, D. Zeng, K. Xu, J. Cui, X. Li, and G. Wang, "Synthesis and characterization of a novel magnetic chitosan microsphere for lactase immobilization," *Colloids and Surfaces A: Physicochemical and Engineering Aspects*, vol. 606, article 125522, 2020.